Int J Thermophys (2008) 29:158–170
DOI 10.1007/s10765-007-0331-7

Impurity Effect in Silver-Point Realization

J. V. Widiatmo · K. Harada · K. Yamazawa · M. Arai

Published online: 30 January 2008

Abstract CCT-WG1 has recommended the sum of individual estimates (SIE) method to correct for the influence of impurities on the realization of temperature fixed points when a detailed impurity analysis is available. The method to estimate the uncertainty of the SIE has also been reported. On the other hand, most cells are fabricated from commercial fixed-point metals that often have no detailed impurity analysis, so the SIE calculation is impossible in that case. Due to this circumstance, and with the focus on the silver fixed point, a new fixed-point cell was fabricated in such a way that a portion of the silver ingot used was extractable during the silver casting. This portion was then analyzed by glow discharge mass spectrometry (GDMS), and the result used to calculate the SIE correction and its uncertainty. Temperature measurements during melting and freezing were collected using new and existing silver fixed-point cells under various conditions. These measurements were used to derive the slope of the silver freezing curve, from which the effect of impurities was evaluated by thermal analysis. The difference between the SIE and the thermal analysis method was evaluated to check the inaccuracy of the thermal analysis from the SIE point of view.

Keywords Continuous freezing · Fixed point · Freezing-point impurity · Sum of individual estimates

J. V. Widiatmo (✉) · K. Harada · K. Yamazawa · M. Arai
Thermometry Section, Temperature and Humidity Division, National Metrology Institute of Japan, AIST, AIST Tsukuba Central 3, Umezono 1-1-1, Tsukuba, Ibaraki 305-8563, Japan
e-mail: janu-widiatmo@aist.go.jp

1 Introduction

Recently, the Consultative Committee for Thermometry's Working Group 1 (CCT-WG1) recommended the use of the sum of individual estimates (SIE) method to correct for the influence of impurities on the realization of temperature fixed points when a detailed impurity analysis is available [1]. The method to derive the uncertainty of the SIE correction has also been reported [2]. However, most cells used to realize the fixed points are made from commercially available fixed-point metals that have no detailed impurity analysis, and so calculation of the SIE correction is impossible.

Due to the above circumstance, a new silver fixed-point cell was fabricated so that part of the silver sample could be extracted during the casting of the silver into its crucible. This sample was then analyzed by glow discharge mass spectrometry (GDMS) and the result used to calculate the SIE correction and its uncertainty.

Temperature measurements of the new silver-point cell during melting and freezing were collected under various conditions following what are called outer-mantle procedures and were used to derive the slope of the silver freezing curve. The same measurements were also carried out with existing silver cells whose fixed-point metals have no impurity analysis.

Finally, the difference between the SIE and the thermal analysis was evaluated to see the inaccuracy (or applicability) of the thermal analysis from the SIE point of view.

2 Apparatus

To realize the silver-point (961.78 °C), a silver fixed-point cell and a suitable furnace are required. We have some silver cells whose 6N nominal purity ingots have no detailed impurity analysis. In the following subsections, the fabrication of additional silver cells and the fixed-point furnace are outlined.

2.1 Fixed-Point Cells

Fixed-point cells, including both the newly fabricated and existing ones, consist of a graphite crucible with a graphite cap within which the silver ingot is enclosed, a graphite thermometer well and its graphite holder to fix the well in the center of the crucible, a quartz thermometer well that is placed in the graphite thermometer well, graphite wool to provide thermal insulation, some platinum sheets supported by graphite disks to minimize the loss of heat by radiation, a quartz cylinder to enclose all the parts, and a cap to seal the inner part of the quartz cylinder. The cylinder cap is equipped with a gas port, enabling pressurization or evacuation of the cylinder. The fixed-point cell is illustrated in Fig. 1.

Commercially available silver powder of 5N5 nominal purity (Ishifuku Metal Industry, Lot No. 03-08-01) was used to fabricate one silver cell through the metal filling method reported elsewhere [3], except that the silver powder was first baked to eliminate possible impurities on the powder surface prior to it being melted into the crucible. In order to be able to analyze the silver after the metal filling, a modification to the reported filling method [3] was introduced. A special graphite funnel was prepared

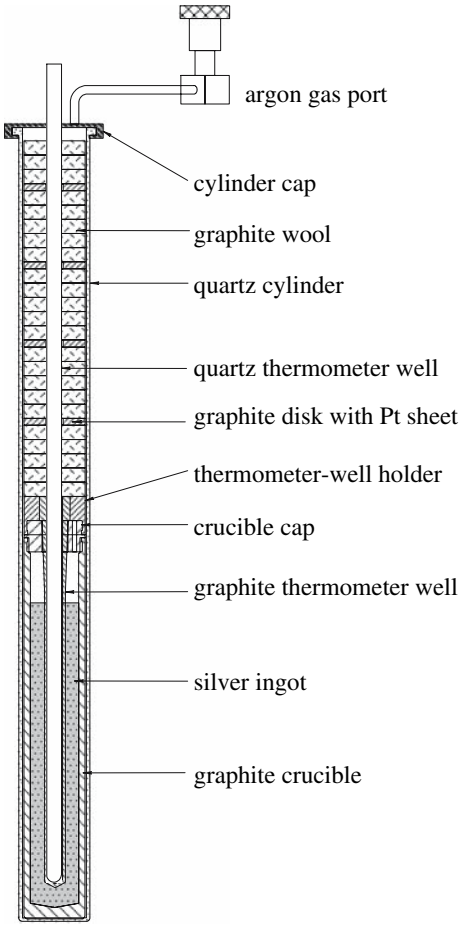

Fig. 1 Setup of silver-point cell

and fixed on the graphite crucible to provide a space adequate to cast the whole silver ingot. Such an assembly is illustrated in Fig. 2a. This assembly was heated in a furnace to melt the silver shot. The completely melted silver shot in the graphite funnel passed through the mouth of the funnel to the lower part of the crucible. The mouth of the funnel was made in such a way that a small portion of melted silver pooled in a nearby area. When the assembly cooled, a small silver ingot was left near the funnel mouth as illustrated in Fig. 2b. This small ingot was then analyzed using GDMS [4]. Graphite weights were then used to push the graphite thermometer well down into the silver ingot as it melted within the crucible inside the closed quartz cylinder (see Fig. 2c, d). Two attempts were made using this modified method to check for possible variation in the impurity analyses. One lot of commercial silver shot (6N nominal purity, Johnson–Matthey, Lot No. A25Q24) was used for these trials.

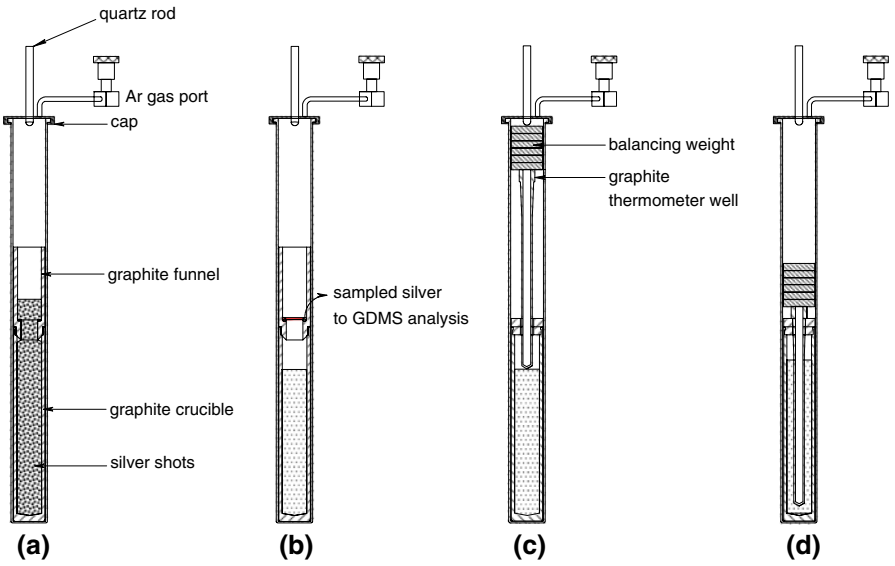

Fig. 2 Method of filling high purity silver into the crucible

2.2 Fixed-Point Furnaces

An existing furnace and a newly fabricated one were used in the present work. Both furnaces have a sodium heat pipe, with the existing one having an electrical heater directly wound on the heat pipe while the heat pipe of the new furnace is enclosed in an Inconel basket on which the electrical heater is wound. Temperature control of the existing furnace is done with the aid of an R-type thermocouple whose reference junction is maintained at the ice point. The new furnace is controlled by means of a platinum-sheathed PRT coupled to a resistance bridge [5,6]. The use of the PRT + bridge combination has refined the temperature control of the new furnace compared to the existing one. Figure 3 compares the temperature stability of the furnaces near 950°C and shows the significant improvement with the new furnace. The temperature was measured by an SPRT fully immersed in the thermometer well of a silver cell within the furnaces.

The temperature control of the furnace was also evaluated through the response of the heater and heat pipe to a change in the temperature setting. A set of temperature values was programmed and executed with the furnace with a silver cell installed. During the execution of the program, an SPRT inserted into the quartz thermometer well of the silver cell measured the temperature. Figure 4 shows the programmed temperature value and the measured temperature. Although a delay was detected between the programmed and measured temperatures, the temperature controls in both the existing and new furnaces satisfactorily realized the programmed temperature. Figure 4 shows that the delay of the new furnace is longer than that of the existing one. This may be due to the presence of the Inconel basket used to contain the sodium heat pipe in the new furnace.

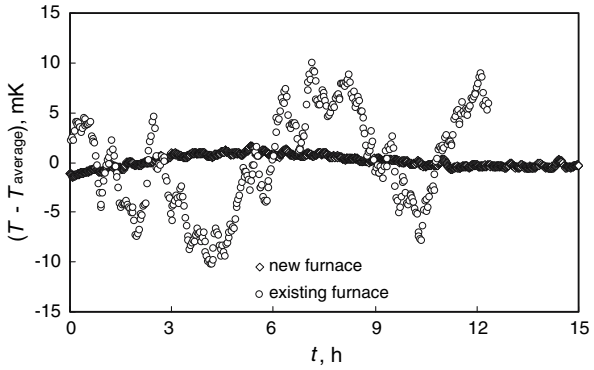

Fig. 3 Temperature stability of existing and newly made furnaces

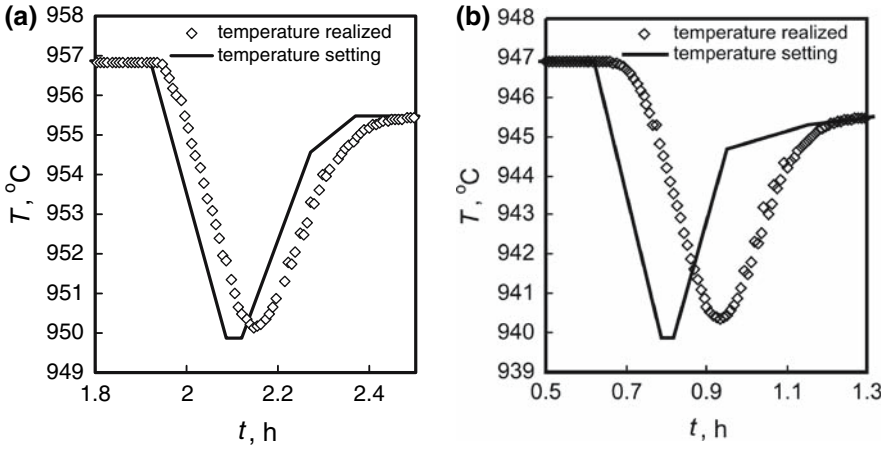

Fig. 4 Response of temperature control in the (**a**) existing and (**b**) newly made furnaces

3 Measurements

The silver fixed point was realized in the present work through solidification of melted silver in the fixed-point cell. Solidification is generally induced by inserting a rod into the quartz thermometer well, causing nucleation also to take place on the outer wall of the thermometer well, as recommended in the Supplementary Information of the ITS-90 [7] (forming inner and outer mantles—a double mantle—in the crucible during freezing). In this work, nucleation was created only by adjusting the furnace temperature, so the solid–liquid interface is expected to begin at the crucible wall (forming an outer mantle) and move inward to the thermometer well as solidification progresses. This nucleation method was adopted to determine more accurately the liquid fraction during freezing. Introduction of any cold object into the thermometer well would cause the liquid fraction determination to be less accurate. Arai and Harada [8] evaluated the realization of aluminum based on the outer-mantle method and reported that no significant difference in the realized temperature was detected between the

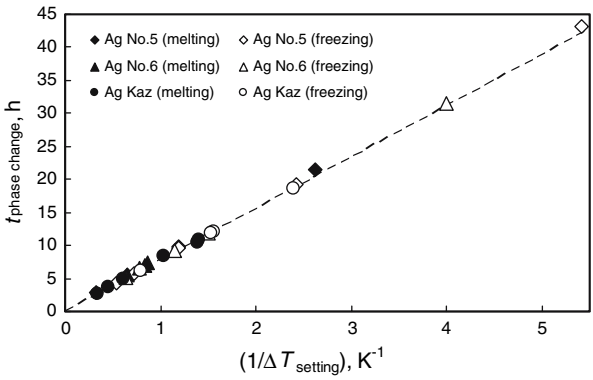

Fig. 5 Phase-change time in terms of the rate of solidification

double-mantle and the outer-mantle methods. They also adopted the outer-mantle method to realize the silver-point and reported very good repeatability.

The nucleation started from a temperature $T_{\text{Ag}}+1\,\text{K}$, where T_{Ag} is the silver freezing point, and the following procedure was carried out:

1. Reduce the furnace temperature from $T_{\text{Ag}} + 1\,\text{K}$ to $T_{\text{Ag}} - 6\,\text{K}$ in 10 min, during which super cooling occurs, followed by temperature recalescence.
2. Maintain the temperature at $T_{\text{Ag}} - 6\,\text{K}$ for 3 min, and then increase it to $T_{\text{Ag}} - 1.3\,\text{K}$ in 9 min.
3. Increase the furnace temperature to $T_{\text{Ag}} - 0.4\,\text{K}$ at a rate of $0.15\,\text{K}\cdot\text{min}^{-1}$, and then change it to the desired final furnace temperature, T_{setting}, at the same rate.

Based on the above nucleation procedure, the time required for the phase change (phase-change time) during melting and freezing was measured using the existing and the newly fabricated silver cells with both the existing and new furnaces. Referring to Fig. 4 where the programmed temperature is realized satisfactorily by the furnace, it is possible to correct the phase-change time for the amount of metal solidified during recovery from the super cooled state. Figure 5 represents the phase-change time, $t_{\text{phase change}}$, measured at various T_{setting} values using three silver cells in the new furnace. $\Delta T_{\text{setting}}$ in the abscissa of Fig. 5 is written as $|T_{\text{setting}} - T_{\text{Ag}}|$. The legend indicates the symbols used to identify the cells and the condition under which the measurements were made, namely, during melting (closed symbols) or freezing (open symbols). The line shows the tendency of the data plots. The data with open symbols has been corrected for the influence of super cooling. If the open data points are compared with the closed ones, a similar tendency can be seen in Fig. 5, implying that the correction of the freeze is reliable. As confirmation, a measurement was made where the furnace temperature was programmed to remelt the silver mantle after the usual nucleation procedure. The phase-change time of this melting process will be equivalent to the corresponding phase-change time attributed to the nucleation process. On the other hand, the phase-change time can also be calculated on the basis of Fig. 5. By comparing both phase-change times, they were found to be in good agreement.

Since the three cells have silver of almost the same mass and are of nearly identical cell design, they show very similar behavior. It can be seen from Fig. 5 that the greater

the $\Delta T_{\text{setting}}$, the shorter the $t_{\text{phase change}}$ will be. In other words, $\Delta T_{\text{setting}}$ reflects the rate of solidification. Although Fig. 5 only shows the case for the new furnace, similar results were also obtained for the existing furnace.

4 Thermal Analysis

In the present work, the phase change is realized by fixing the furnace temperature some degrees above (in the case of melting) or below (in the case of freezing) the silver freezing point. Under that condition, a portion of heat is constantly added (or rejected) to the silver and a corresponding mass of silver is constantly melted (or frozen). From this, the fraction of liquid silver, usually denoted by F, can be assumed to be equivalent to the ratio of time at any point during the phase change to the total time required for the complete phase change. For confirmation, the heater power was measured during melting and freezing. The method to measure the heater power was the same as that adopted for our work with tin [9]. Results similar to those for tin were obtained; the heater power was almost constant during the phase transition, implying that heat was almost constantly added to (or rejected from) the silver. In other words, F changed at an almost constant rate. The monitoring of the heater power also confirmed the points of change during the phase transition, i.e., the start of melting, the melt-off point, the end of nucleation, and the end of freezing.

Figure 6 shows one of the freezing curves obtained from measurements in the present section, displayed as a function of $1/F$. The ordinate is the resistance ratio, W, of the resistance thermometer. There is a range, below $1/F = 2.5$, in the freezing curve where the data forms a straight line; the slope of the line is the steepest part of the curve. Since the measurements during the phase change as described in the previous section were done at various $\Delta T_{\text{setting}}$, it is possible to arrange the slope of the freezing curves in terms of $\Delta T_{\text{setting}}$.

The dependence of the slope of the freezing curves on the rate of solidification for the silver cells used in the present work is presented in Fig. 7. The silver cells are listed in Table 1. The legend of the figure identifies the cell and the type of resistance thermometer used for the measurements. PRT in the legend stands for a Pt-sheathed PRT (Netsushin HTS series [5]). Measurements using cell Ag No. 5 were made with a

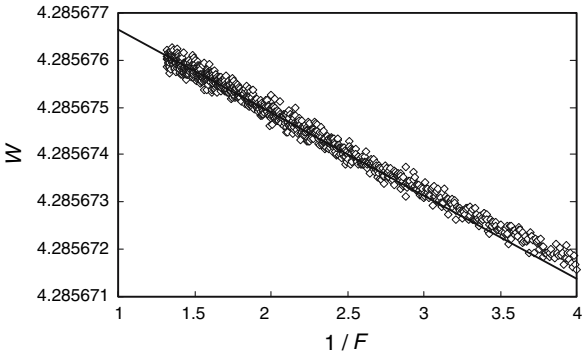

Fig. 6 Freezing curve in terms of $1/F$

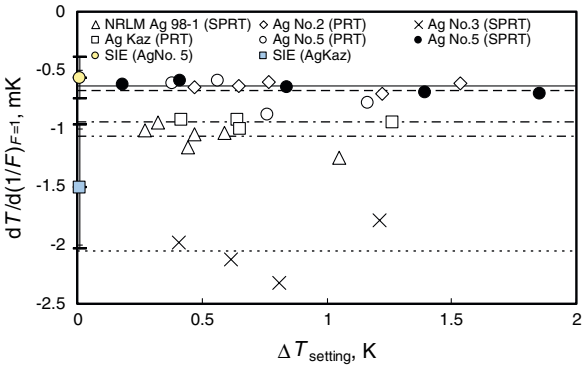

Fig. 7 Freezing curve slope in terms of rate of solidification and the SIE

Table 1 Silver fixed-point cells studied in the present work

Cell	Mass of ingot (g)	Size	Nominal purity	Supplier
NRLM Ag 98-1[a]	1800	Shots	6N	JM[b]
Ag No. 2	1887	Shots	6N	JM[b]
Ag No. 3	1750	Powder	5N5	IMI[c]
Ag No. 5	1750	Shots	6N	JM[b]
Ag Kaz	1750	Shots	6N	JM[b]

[a]Used for the CCT-K4 international comparison
[b]Johnson Matthey
[c]Ishifuku Metal Industry

SPRT and a PRT to check for any dependence on the thermometer. Figure 7 indicates that there is no significant dependence on the measuring thermometer. From the data in the figure, no dependence of the slope of the freezing curve on the rate of solidification can be detected. Since the rate of solidification is also related to the heat flux during freezing, it can be said that the slope of the freezing curve is independent of the heat flux. The slope of cell Ag No. 3 of 5N5 nominal purity is steeper than that of the cells having 6N nominal purity. The slope may reflect the quality (purity) of the cell. Among cells that have 6N silver, namely, cells NRLM Ag 98-1, Ag No. 2, Ag No. 5, and Ag Kaz, two groups of slope values were observed. Cells NRLM Ag 98-1 and Ag Kaz are in one group whose slope is steeper than the group with cells Ag No. 2 and Ag No. 5. The difference in slope is about 0.5 mK. Figure 7 may represent the typical quality of commercially available 6N silver, noting that the 6N silver samples were purchased from one manufacturer. It is interesting to quote the work by Ancsin [10] who reported that the liquidus points of his four 6N silver samples differed from that of ideally pure silver by no more than 1.0 mK. The melting points of these samples were realized within a scatter band of ±0.55 mK. By chance, Ancsin purchased the samples from the same manufacturer.

5 Sum of Individual Estimates

The silver samples used in the present work with relatively detailed impurity analyses are those for cells Ag No. 3 and Ag No. 5. The manufacturer's reported analysis was obtained using ICPMS. Cell Ag No. 3 was fabricated using our method as reported elsewhere [3], while cell Ag No. 5 used the modified one described in Sect. 2. The silver sample left after the filling of cell Ag No. 5 was analyzed using GDMS [4]. Such sampling was also done using the rest of silver from the lot used for cell Ag No. 5. The impurity analyses of both samples showed a sample-to-sample variation in impurity concentration of some tens of ppb. Since some of the silver shot used in cell Ag Kaz were available, they were also analyzed using GDMS [4]. It should be noted that this shot was stored for two years after the cell fabrication, so contamination during that period may have occurred.

Table 2 lists the impurity elements detected in the various silver samples. For Ag No. 5, besides the elements detected by ICPMS, the manufacturer also provided the detection limits for the other elements. Of the elements detected before (by ICPMS) and after (by GDMS) the silver casting process, Fe was detected in both cases, and there is a relative difference of about 30% between the two concentration values. Although the value after the filling process is higher than that before, considering that the typical expanded uncertainty ($k = 2$) of GDMS is within a factor of two of the values obtained [10], there is no evidence to suggest that contamination occurred during the silver filling process.

Using the values listed in Table 2, it is possible to estimate the departure of the realized silver freezing temperature from the ideal one. A recommended estimation method is the SIE [1] method that is derived from the dependence of the observed equilibrium freezing temperature, T_{obs}, on the fraction of liquid sample, F [1], as

$$T_{\mathrm{obs}} - T_{\mathrm{pure}} = \sum_{\mathrm{i}} c_{\mathrm{l}i} \left(\frac{\partial T}{\partial c_{\mathrm{l}i}}\right) F^{k_{0,i}-1} = \sum_{i} c_{\mathrm{l}i} \left(\frac{\partial T}{\partial c_{\mathrm{l}i}}\right) \left(\frac{1}{F}\right)^{1-k_{0,i}} \tag{1}$$

T_{pure} stands for the freezing temperature of ideally pure fixed-point metal, and $c_{\mathrm{l}i}$, $(\partial T/\partial c_{\mathrm{l}i})$, and $k_{0,i}$ are the concentration of impurity i in equilibrium liquid, the slope of the liquidus line in the phase diagram with respect to $c_{\mathrm{l}i}$, and the equilibrium distribution coefficient of i, respectively. Since the liquidus point is defined as the equilibrium freezing temperature at $F = 1$, Eq. 1 yields Eq. 2 for the SIE and Eq. 3 for the standard uncertainty of the SIE.

$$\Delta T_{\mathrm{SIE}} = T_{\mathrm{obs}} - T_{\mathrm{pure}} = \sum_{\mathrm{i}} c_{\mathrm{l}i} \left(\frac{\partial T}{\partial c_{\mathrm{l}i}}\right) \tag{2}$$

$$u^2\left(\Delta T_{\mathrm{SIE}}\right) = \sum_{\mathrm{i}} \left[u\left(c_{\mathrm{l}i}\right)\left(\frac{\partial T}{\partial c_{\mathrm{l}i}}\right)\right]^2 + \left[c_{\mathrm{l}i} u\left(\frac{\partial T}{\partial c_{\mathrm{l}i}}\right)\right]^2 \tag{3}$$

Table 2 Impurities in the silver fixed-point cells studied in the present work

Element	Ag No. 3 (5N5 purity)	Ag No. 5 (6N purity)		Ag Kaz (6N purity)	$\partial T/\partial c_{li}$ (mK/mass fraction)	$k_{0,i}$
	Mass fraction[a] (µg/g)	Mass fraction[a] (µg/g)	Mass fraction[b] (µg/g)	Mass fraction[b] (µg/g)		
Na	1.2			0.01	−3.5	0.01
Mg	0.11	0.2		0.01	−2.0	0.545
Al	0.26			0.15	−2.6	0.59
Si	0.05			0.15	−3.1	0.285[e]
P			0.08		−2.7	0.007
S			0.03	0.02	−3.1	0.024
Cl			0.14	0.25		
Ca	0.73			0.05	−3.7	0.217[e]
Ti				0.01	−0.01	0.964
V				0.01		
Cr	0.073		0.07	0.1		
Mn			0.002	0.03	0.15	>>1
Fe	1.1	0.3	0.41	1.5	0.13[c]	1.06[d]
Co	0.032	0.2		0.03	2.0	2.5
Ni	0.1		0.01	0.15	−0.74[c]	0.623
Cu	0.12		0.02	0.07	−0.69[c]	0.4
Zn	0.15		0.05	0.02	−1.10[c]	0.45
Se			0.06	0.15	−2.7	0.077
Rh	0.42					
Cd	0.09				−0.34	0.565
Sn			0.03	0.1	−0.60[c]	0.205
Sb			0.08	0.33	−0.73[c]	0.253
Ir	0.33				−0.19	0.333
Pt	0.01			0.3	1.3	2.174
Au	0.1				0.09[c]	1.05
Pb	0.01			0.1	−0.48[c]	0.277
Bi	0.02			0.05	−0.63	0.099

[a] From ICP MS
[b] From GDMS
[c] Ancsin [9]
[d] Derived from Ancsin [9]
[e] Derived from Eq. 4

Table 3 SIE for silver fixed-point cells studied in the present work

Cell	SIE (mK)	u(SIE) (mK)
Ag No. 3	−8.16	2.95
Ag No. 5	−0.57	0.18
Ag Kaz	−1.50	0.53

The values of $\partial T/\partial c_{\mathrm{l}i}$ in Eqs. 2 and 3 can be taken from the data compiled by Masaalski et al. [11]. Data for some binary alloys were recently reported by Ancsin [10]. A significant deviation is observed for the Ag+Fe binary alloy. The phase diagram in [11] indicates the possibility of a silver-point depression due to the presence of Fe, while experiments by Ancsin [10] produced a silver-point elevation. This leads to doubt regarding the reliability of $\partial T/\partial c_{\mathrm{l}i}$. In this work, all experimental $\partial T/\partial c_{\mathrm{l}i}$ values reported by Ancsin [10] are adopted as listed in Table 2. The values for other binary alloys are taken from reference [11]. Also tabulated in Table 2 are the $k_{0,i}$ derived from Ref. [11], except that for Ag+Fe, which is calculated from the experimental $\partial T/\partial c_{\mathrm{l}i}$ and the relationship,

$$\frac{\partial T}{\partial c_{\mathrm{l}i}} = -\frac{1-k_{0,i}}{A} \tag{4}$$

that is valid at low concentrations [1]. A in Eq. 4 is the cryoscopic constant.

The standard uncertainty of the SIE, u(SIE), can be calculated following the method proposed by Fellmuth and Hill [2], namely, by taking half of the concentration values or half of the detection limit as the uncertainties of the analysis results, $u(c_{\mathrm{l}i})$, and a relative uncertainty of order 30% for $u(\partial T/\partial c_{\mathrm{l}i})$ which comes from the greatest difference, except for the Ag+Fe case, between Ref. [11] and the values reported by Ancsin [10]. Table 3 shows the SIE corrections for cells Ag No. 3, Ag No. 5, and Ag Kaz along with their standard uncertainties.

6 Discussion

The slopes of the freezing curves in Fig. 7 are grouped according to the purity of silver in the fixed-point cells. This fact promotes the use of the slope of the freezing curve as a means to evaluate the quality of the cell. It is interesting to see how much this slope departs from the SIE calculation. This evaluation using the slope of the freezing curve is termed thermal analysis hereafter for convenience.

The slope of the freezing curve (at $F = 1$) can be derived from Eq. 1 to obtain Eq. 5.

$$\left[\frac{\partial\left(T_{\mathrm{obs}}-T_{\mathrm{pure}}\right)}{\partial\left(1/F\right)}\right]_{F=1} = -\sum_{\mathrm{i}} c_{\mathrm{l}i}\left(k_{0,i}-1\right)\left(\frac{\partial T}{\partial c_{\mathrm{l}i}}\right) \tag{5}$$

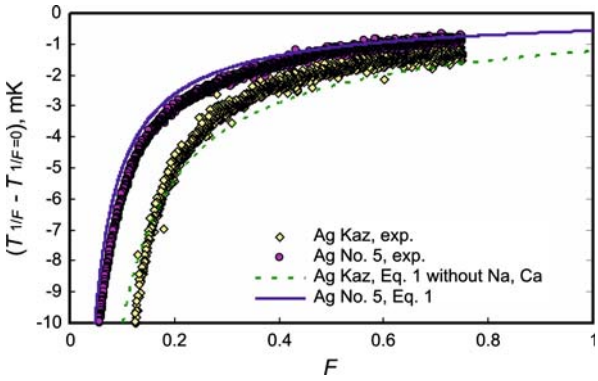

Fig. 8 Theoretical and experimental freezing curves

The thermal analysis represented by Eq. 5 differs from Eq. 2 for the SIE method by a factor $-(k_{0,i} - 1)$. For $k_{0,i} < 1$, $\partial T/\partial c_{\mathrm{l}i} < 1$, while for $k_{0,i} > 1$, $\partial T/\partial c_{\mathrm{l}i} > 1$; hence, the slope of the freezing curve will always be negative. For samples with only $k_{0,i} > 1$ elements, thermal analysis will give values of opposite sign to the SIE.

Figure 7 also compares the thermal analysis to the SIE, along with its uncertainty (shown by the error bar), as listed in Table 3. For cell Ag No. 5, whose impurity analysis was conducted using part of the silver collected during filling, the thermal analysis agrees with the SIE within the uncertainty, u(SIE). On the other hand, for cell Ag Kaz, thermal analysis shows greater departure from the SIE, and cell Ag No. 3 departs even more. Noting that their analyses were done prior to the silver filling, the concentrations of certain elements, especially those with relatively low normal boiling points, may have "decreased" while baking under vacuum prior to the filling described in Sect. 2.1, altering the freezing curve from what was predicted. Na and Ca, the two elements with the largest $\partial T/\partial c_{\mathrm{l}i}$ among the elements listed in Table 2, are predicted to decrease in concentration during baking due to their relatively high vapor pressures at the silver point (197 kPa [12] and about 1.0 kPa [13], respectively). This case would be especially significant for Ag No. 3 which was fabricated from silver powder.

Besides the SIE calculation, Table 2 can also be used to plot a theoretical freezing curve by means of Eq. 1. Figure 8 shows the theoretical and experimental freezing curves for cells Ag No. 5 and Ag Kaz, excluding Na and Ca. $T_{1/F}$ and $T_{1/F=0}$ in the ordinate correspond to T_{obs} and T_{pure} in Eq. 1. The hypothetical temperature $T_{1/F=0}$ is derived from the slope of the freezing curve. In the case of cell Ag No. 5, the experimental curve is represented precisely by Eq. 1, even at the end of the solidification process. In the case of Ag Kaz, the theoretical curve shifts closer to the experimental one by excluding Na and Ca. Although not shown in Fig. 8, a similar result is also obtained for Ag No. 3. This may support the hypothesis that the concentrations of certain elements "decreased" during the silver filling process. Despite a factor $-(k_{0,i} - 1)$ that differentiates the thermal analysis from the SIE, Fig. 7 shows that, at least for the 6N silver used in this work, the influence of the factor is within the uncertainty of the SIE. This suggests the possible application of thermal analysis to estimate the influence of impurities on the realization of the silver-point.

To confirm the consistency of the thermal analysis, a direct comparison of the silver cells is essential. Such comparisons have been recommended by some authors to evaluate the effect of impurities; the method is referred to as an estimation based on representative cell comparisons (ERC)—but this method is not recommended by CCT-WG1. However, for the silver-point work reported here, an SPRT whose change in resistance at the triple point of water after soaking at the silver point is smaller than, say, 0.5 mK would be necessary. Such a SPRT should also be stable when it is moved from one cell to another at the silver-point temperature. A reliable silver-cell comparison becomes our challenge for the future whenever an SPRT with high thermal stability becomes available.

Acknowledgments The authors are indebted to Mr. Yuichiro Shindo from Nippon Mining and Metals Co., Ltd. (formerly Nikko Materials Co., Ltd.) for conducting impurity analyses on some of the samples used in the present study.

References

1. D. Ripple, B. Fellmuth, M. de Groot, Y. Hermier, K.D. Hill, P.P.M. Steur, A. Pokhodun, M. Matveyev, P. Bloembergen, CCT Document **CCT/05-08** (2005)
2. B. Fellmuth, K.D. Hill, Metrologia **43**, 71 (2006)
3. J.V. Widiatmo, K. Harada, K. Yamazawa, M. Arai, Metrologia **43**, 561 (2006)
4. Y. Shindo, *Personal communication* (2006)
5. M. Arai, A. Kawata, T. Imamura, K. Kinoshita, in *Temperature: Its Measurement and Control in Science and Industry*, vol. 7, ed. by D.C. Ripple (AIP, New York, 2003), pp. 357–361
6. M. Arai, K. Yamazawa, *Proceedings of SICE Annual Conference 2004* (SICE, Tokyo 2004), pp. 1172–1175
7. H. Preston-Thomas, P. Bloembergen, T.J. Quinn, *Supplementary Information for the International Temperature Scale of 1990*, BIPM (1990)
8. M. Arai, K. Harada, Netsu Bussei **13**, 258 (1999)
9. K. Yamazawa, J.V. Widiatmo, M. Arai, in *Proceedings of TEMPMEKO 2007*, Int. J. Thermophys. **28**, 1941 (2007) DOI: 10.1007/s10765-007-0280-1
10. J. Ancsin, Metrologia **38**, 229 (2001)
11. T.B. Massalski, H. Okamoto, P.R. Subramanian, L. Kacprzak, *Binary Alloy Phase Diagrams*, 2nd edn., vol. 1 (ASM International, 1990)
12. K.D. Hill, M. Gotoh, Metrologia **33**, 49 (1996)
13. G. De Maria, V. Piacente, J. Chem. Thermodyn. **6,** 1 (1974)